

Non extensive thermodynamics and neutron star properties

Débora P. Menezes,¹ Airton Deppman,² Eugenio Megías,^{3,4} and Luis B. Castro⁵

¹*Departamento de Física - CFM - Universidade Federal de Santa Catarina,
Florianópolis - SC - CP. 476 - CEP 88.040 - 900 - Brazil
email: debora.p.m@ufsc.br*

²*Instituto de Física, Universidade de São Paulo - Rua do Matão Travessa
R Nr.187 CEP 05508-090 Cidade Universitária, São Paulo - Brasil
email: deppman@if.usp.br*

³*Grup de Física Teòrica and IFAE, Departament de Física,
Universitat Autònoma de Barcelona, Bellaterra E-08193 Barcelona, Spain*

⁴*Max-Planck-Institut für Physik (Werner-Heisenberg-Institut),
Föhringer Ring 6, D-80805, Munich, Germany
email: emegias@mpp.mpg.de*

⁵*Departamento de Física, Universidade Federal do Maranhão,
Campus Universitário do Bacanga, CEP 65080-805, São Luís, MA, Brazil
email: lrb.castro@ufma.br*

In the present work we apply non extensive statistics to obtain equations of state suitable to describe stellar matter and verify its effects on microscopic and macroscopic quantities. Two snapshots of the star evolution are considered and the direct Urca process is investigated with two different parameter sets. q -values are chosen as 1.05 and 1.14. The equations of state are only slightly modified, but the effects are enough to produce stars with slightly higher maximum masses. The onsets of the constituents are more strongly affected and the internal stellar temperature decreases with the increase of the q -value, with consequences on the strangeness and cooling rates of the stars.

PACS numbers: 05.70.Ce, 21.65.-f, 26.60.-c, 95.30.Tg

I. INTRODUCTION

A type II supernova explosion is triggered when massive stars ($8 M_{\odot} < M < 30 M_{\odot}$) exhaust their fuel supply, causing the core to be crushed by gravity. The remnant of this gravitational collapse is a compact star or a black hole, depending on the initial condition of the collapse. Newly-born protoneutron stars (PNS) are hot and rich in leptons, mostly e^{-} and ν_e and have masses of the order of $1 - 2 M_{\odot}$ [1, 2]. During the very beginning of the evolution, most of the binding energy, of the order of 10^{53} ergs is radiated away by the neutrinos. During the temporal evolution of the PNS in the so-called Kelvin-Helmholtz epoch, the remnant compact object changes from a hot and lepton-rich PNS to a cold and deleptonized neutron star [3]. The neutrinos already present or generated in the PNS hot matter escape by diffusion because of the very high densities and temperatures involved. At zero temperature no trapped neutrinos are left in the star because their mean free path would be larger than the compact star radius. Simulations have shown that the evolutionary picture can be understood if one studies three snapshots of the time evolution of a compact star in its first minutes of life [4]. At first, the PNS is warm (represented by fixed entropy per particle) and has a large number of trapped neutrinos (represented by fixed lepton fraction).

As the trapped neutrinos diffuse, they heat up the star. Finally, the star is considered cold.

To describe these three snapshots, appropriate equations of state (EOS) have to be used. These EOS are normally parameter dependent and are adjusted so as to reproduce nuclear matter bulk properties, as the binding energy at the correct saturation density and incompressibility as well as ground state properties of some nuclei [5–7]. Until recently, when two stars with masses of the order of $2M_{\odot}$ were confirmed [8, 9], most EOS were expected to produce maximum stellar masses just larger than $1.44M_{\odot}$ and radii of the order of 10 to 13 km. The new measurements imposed more rigid constraints on the EOS.

On the other hand, the effects of non extensive statistical mechanics [10] have been explored both in high-energy physics [11, 12] and astrophysical problems [13]. The q -deformed entropy functional that underlines non extensive statistics depends on a real parameter (q) that determines the degree of nonadditivity of the functional and in the limit $q \rightarrow 1$, it becomes additive and the standard Boltzmann-Gibbs entropy is recovered.

In the present work we investigate how the consideration of non extensive statistics affects hadronic matter at finite temperature and large densities by applying it to PNS. Based on an extensive study of parameter dependent relativistic models [14] and on the mentioned $2M_{\odot}$ stars, we have opted to work with two parametrizations of the non-linear Walecka model [5], namely GM1 [15] and IUFSU [16]. Hence, we also check how parameter dependent the stellar matter microscopic (EOS, particle fractions, strangeness, internal temperature, direct Urca process onset) and macroscopic (radius, gravitational and baryonic masses, central energy density) properties are when Tsallis statistics is used.

The work is organized as follows: in Section II, the basic equations necessary to follow the EOS calculations both with standard hadrodynamics and with non extensive statistics are outlined. In Section III our results are displayed and discussed, and finally the main conclusions are drawn in Section IV.

II. THE FORMALISM

A. Standard quantum hadrodynamics

In this section we present the hadronic equations of state (EOS) used in this work. We describe hadronic matter within the framework of the relativistic non-linear Walecka model (NLWM) [5]. In this model the nucleons are coupled to neutral scalar σ , isoscalar-vector ω_{μ} and isovector-vector $\vec{\rho}_{\mu}$ meson fields. We also include a $\rho - \omega$ meson coupling term as in [16–18] because it was shown to have important consequences in neutron star properties related to the symmetry energy and its slope [19].

The Lagrangian density reads

$$\begin{aligned}
\mathcal{L} = & \sum_j \bar{\psi}_j \left[\gamma_\mu (i\partial^\mu - g_{\omega j} \omega^\mu - g_{\rho j} \vec{\tau}_j \cdot \vec{\rho}^\mu) - m_j^* \right] \psi_j \\
& + \frac{1}{2} \partial_\mu \sigma \partial^\mu \sigma - \frac{1}{2} m_\sigma^2 \sigma^2 - \frac{1}{3!} k \sigma^3 - \frac{1}{4!} \lambda \sigma^4 \\
& - \frac{1}{4} \Omega_{\mu\nu} \Omega^{\mu\nu} + \frac{1}{2} m_\omega^2 \omega_\mu \omega^\mu + \frac{1}{4!} \xi g_\omega^4 (\omega_\mu \omega^\mu)^2 \\
& - \frac{1}{4} \vec{R}_{\mu\nu} \cdot \vec{R}^{\mu\nu} + \frac{1}{2} m_\rho^2 \vec{\rho}_\mu \cdot \vec{\rho}^\mu \\
& + \Lambda_v (g_\rho^2 \vec{\rho}_\mu \cdot \vec{\rho}^\mu) (g_\omega^2 \omega_\mu \omega^\mu) \\
& + \sum_l \bar{\psi}_l (i\gamma_\mu \partial^\mu - m_l) \psi_l, \tag{2.1}
\end{aligned}$$

where

$$m_j^* = m_j - g_{\sigma j} \sigma \tag{2.2}$$

is the baryon effective mass, $\Omega_{\mu\nu} = \partial_\mu \omega_\nu - \partial_\nu \omega_\mu$, $\vec{R}_{\mu\nu} = \partial_\mu \vec{\rho}_\nu - \partial_\nu \vec{\rho}_\mu - g_\rho (\vec{\rho}_\mu \times \vec{\rho}_\nu)$, $g_{ij} = X_i g_i$ are the coupling constants of mesons $i = \sigma, \omega, \rho$ with baryon j , m_i is the mass of meson i and l represents the leptons e^- and μ^- and respective neutrinos. The couplings k ($k = 2 M_N g_\sigma^3 b$) and λ ($\lambda = 6 g_\sigma^4 c$) are the weights of the non-linear scalar terms and $\vec{\tau}$ is the isospin operator. The sum over j in (2.1) can be extended over neutrons and protons only or over the lightest eight baryons $\{n, p, \Lambda, \Sigma^-, \Sigma^0, \Sigma^+, \Xi^-, \Xi^0\}$. The coupling constants $\{g_{\sigma j}\}_{j=\Lambda, \Sigma, \Xi}$ of the hyperons with the scalar meson σ can be constrained by the hyper-nuclear potentials in nuclear matter to be consistent with hyper-nuclear data [20, 21], but we next consider $X_\sigma=0.7$ and $X_\omega = X_\rho=0.783$ and equal for all the hyperons as in [6]. In Table I we give the symmetric nuclear matter properties at saturation density as well as the parameters of the models used in the present work.

Applying the Euler-Lagrange equations to (2.1), assuming translational and rotational invariance, static mesonic fields and using the mean-field approximation ($\sigma \rightarrow \langle \sigma \rangle = \sigma_0$; $\omega_\mu \rightarrow \langle \omega_\mu \rangle = \delta_{\mu 0} \omega_0$; $\vec{\rho}_\mu \rightarrow \langle \vec{\rho}_\mu \rangle = \delta_{\mu 0} \delta^{i3} \rho_0^3 \equiv \delta_{\mu 0} \delta^{i3} \rho_{03}$), we obtain the following equations of motion for the meson fields:

$$\begin{aligned}
m_\sigma^2 \sigma_0 &= -\frac{k}{2} \sigma_0^2 - \frac{\lambda}{6} \sigma_0^3 + \sum_j g_{\sigma j} n_j^s, \\
m_\omega^2 \omega_0 &= -\frac{\xi g_\omega^4}{6} \omega_0^3 + \sum_j g_{\omega j} n_j - 2\Lambda_v g_\rho^2 g_\omega^2 \rho_{03}^2 \omega_0, \\
m_\rho^2 \rho_{03} &= \sum_j g_{\rho j} \tau_{3j} n_j - 2\Lambda_v g_\rho^2 g_\omega^2 \omega_0^2 \rho_{03}, \tag{2.3}
\end{aligned}$$

where

$$n_j^s = \int \frac{d^3 p}{(2\pi)^3} \frac{m_j^*}{E_j^*} (f_{j+} + f_{j-}), \tag{2.4}$$

is the baryon scalar density of particle j and the respective baryon density

$$n_j = \frac{2}{(2\pi)^3} \int d^3 p (f_{j+} - f_{j-}), \quad n_B = \sum_j n_j, \tag{2.5}$$

and $f_{j\pm}$ is the Fermi distribution for the baryons (+) and anti-baryons (-) j :

$$f_{j\pm} = \frac{1}{e^{\beta(E_j^* \mp \nu_j)} + 1}, \quad (2.6)$$

with $\beta = 1/T$, $E_j^* = (\mathbf{p}_j^2 + m_j^{*2})^{1/2}$ and the effective chemical potential of baryon j is given by

$$\nu_j = \mu_j - g_\omega \omega_0 - \tau_{3j} g_\rho \rho_{03}. \quad (2.7)$$

The EoS can then be calculated and reads:

$$\begin{aligned} P = & \frac{1}{3\pi^2} \sum_j \int \frac{p^4 dp}{\sqrt{p^2 + m_j^{*2}}} (f_{j+} + f_{j-}) + \frac{m_\omega^2}{2} \omega_0^2 \\ & + \frac{\xi}{24} \omega_0^4 + \frac{m_\rho^2}{2} \rho_{03}^2 - \frac{m_\sigma^2}{2} \sigma_0^2 - \frac{k}{6} \sigma_0^3 - \frac{\lambda}{24} \sigma_0^4 + \Lambda_v g_\rho^2 g_\omega^2 \omega_0^2 \rho_{03}^2 \\ & + \frac{1}{3\pi^2} \sum_l \int \frac{p^4 dp}{\sqrt{p^2 + m_l^2}} (f_{l+} + f_{l-}), \end{aligned} \quad (2.8)$$

$$\begin{aligned} \mathcal{E} = & \frac{1}{\pi^2} \sum_j \int p^2 dp \sqrt{p^2 + m_j^{*2}} (f_{j+} + f_{j-}) + \frac{m_\omega^2}{2} \omega_0^2 \\ & + \frac{\xi}{8} \omega_0^4 + \frac{m_\rho^2}{2} \rho_{03}^2 + \frac{m_\sigma^2}{2} \sigma_0^2 + \frac{k}{6} \sigma_0^3 + \frac{\lambda}{24} \sigma_0^4 + 3\Lambda_v g_\rho^2 g_\omega^2 \omega_0^2 \rho_{03}^2 \\ & + \frac{1}{\pi^2} \sum_l \int p^2 dp \sqrt{p^2 + m_l^2} (f_{l+} + f_{l-}), \end{aligned} \quad (2.9)$$

where the lepton distribution functions are given by

$$f_{l\pm} = \frac{1}{e^{\beta(E_l \mp \mu_l)} + 1}, \quad (2.10)$$

with $E_l = (\mathbf{p}_l^2 + m_l^2)^{1/2}$.

The entropy per particle (baryon) can be calculated through the thermodynamical expression

$$\frac{\mathcal{S}}{n_B} = \frac{\mathcal{E} + P - \sum_j \mu_j n_j}{T n_B}. \quad (2.11)$$

When the hyperons are present we define the strangeness fraction:

$$f_s = \frac{1}{3} \frac{\sum_j |s_j| n_j}{n_B}, \quad (2.12)$$

where s_j is the strangeness of baryon j and n_B is the total baryonic density given in eq. (2.5).

| | IU-FSU [16] | GM1 [15] |
|----------------------------------|-------------|-----------|
| n_0 (fm ⁻³) | 0.155 | 0.153 |
| K (MeV) | 231.2 | 300 |
| m^*/m | 0.62 | 0.70 |
| m (MeV) | 939 | 938 |
| $-B/A$ (MeV) | 16.4 | 16.3 |
| \mathcal{E}_{sym} (MeV) | 31.3 | 32.5 |
| L (MeV) | 47.2 | 94 |
| m_σ (MeV) | 491.5 | 512 |
| m_ω (MeV) | 782.5 | 783 |
| m_ρ (MeV) | 763 | 770 |
| g_σ | 9.971 | 8.910 |
| g_ω | 13.032 | 10.610 |
| g_ρ | 13.590 | 8.196 |
| b | 0.001800 | 0.002947 |
| c | 0.000049 | -0.001070 |
| ξ | 0.03 | 0 |
| Λ_v | 0.046 | 0 |

TABLE I: Parameter sets used in this work and corresponding saturation properties.

B. Non extensive statistics

We next give the main formulae necessary for the development and application of the non-extensive formalism to hadronic matter (fermions only) as in [24–26]. They are the exponential function defined as

$$\begin{cases} e_q^{(+)}(x) = [1 + (q - 1)x]^{1/(q-1)} & , x \geq 0, \\ e_q^{(-)}(x) = \frac{1}{e_q^{(+)}(|x|)} = [1 + (1 - q)x]^{1/(1-q)} & , x < 0, \end{cases} \quad (2.13)$$

and the q -logarithm, which reads:

$$\begin{cases} \log_q^{(+)}(x) = \frac{x^{q-1}-1}{q-1}, \\ \log_q^{(-)}(x) = \frac{x^{1-q}-1}{1-q}. \end{cases} \quad (2.14)$$

From the definition of q -deformed entropy [24], we can write the distribution functions:

$$\begin{cases} n_q^{(+)}(x) = \frac{1}{(e_q^{(+)}(x)+1)^q}, \\ n_q^{(-)}(x) = \frac{1}{(e_q^{(-)}(x)+1)^{2-q}}. \end{cases} \quad (2.15)$$

It is worth mentioning that the notation in [13] is different from the one we use and the authors of this paper do not treat the $x < 0$ case correctly. There are some typos in [24], discussed in [25] that were propagated to Ref. [13]. The entropy density reads

$$\mathcal{S} = \begin{cases} \frac{1}{\pi^2} \sum_j \int p^2 dp \left(\frac{x_j}{(e_q^{(+)}(x_j)+1)^q} - \frac{1}{q-1} \left[\left(\frac{e_q^{(+)}(x_j)}{e_q^{(+)}(x_j)+1} \right)^{q-1} - 1 \right] \right) & x_j \geq 0, \\ \frac{1}{\pi^2(q-1)} \sum_j \int p^2 dp \left(-1 + n_q^{(-)}(x_j) + (1 - \tilde{n}_q^{(-)}(x_j))^{2-q} \right) & x_j < 0, \end{cases} \quad (2.16)$$

where we have defined $\tilde{n}_q^{(\pm)}(x) = 1/(e_q^{(\pm)}(x) + 1)$. The pressure is

$$P = \begin{cases} \frac{T}{\pi^{2(q-1)}} \sum_j \int p^2 dp \left[- \left(\frac{e_q^{(+)}(x_j)}{e_q^{(+)}(x_j)+1} \right)^{q-1} + 1 \right] & x_j \geq 0, \\ \frac{T}{\pi^2} \sum_j \int p^2 dp \log_q^{(+)} \left(1 + [e_q^{(-)}(x_j)]^{-1} \right) & x_j < 0 \end{cases} \quad (2.17)$$

the baryonic density

$$n_j = \begin{cases} \frac{1}{\pi^2} \sum_j \int p^2 dp n_q^{(+)}(x_j) & x_j \geq 0, \\ \frac{1}{\pi^2} \sum_j \int p^2 dp n_q^{(-)}(x_j) + 2C_n, & x_j < 0 \end{cases} \quad (2.18)$$

with

$$C_n = \frac{\mu_j T \sqrt{\mu_j^2 - M_j^{*2}} (2^{q-1} + 2^{1-q} - 2)}{2\pi^2 (q-1)} \theta(\mu_j - M_j^*)$$

and the energy density:

$$\mathcal{E} = \begin{cases} \frac{1}{\pi^2} \sum_j \int p^2 dp E n_q^{(+)}(x_j) & x_j \geq 0, \\ \frac{1}{\pi^2} \sum_j \int p^2 dp E n_q^{(-)}(x_j) + 2C_e, & x_j < 0, \end{cases} \quad (2.19)$$

with

$$C_e = \mu_j C_n$$

and where $x_j = \beta(E_j^* - \nu_j)$.

When non extensive statistical mechanics is used instead of the usual Fermi-Dirac expressions for the gas part of the EOS, the expressions for pressure and energy density are rewritten in such a way that the first and last terms in equations (2.8) and (2.9) are substituted by equations (2.17) and (2.19) respectively. Moreover, the usual baryonic density given in eq. (2.5) is replaced by eq. (2.18). In the equations of motion, the scalar density eq. (2.4) is replaced by

$$n_j^s = \begin{cases} \frac{1}{\pi^2} \sum_j \int p^2 dp \frac{m_j^*}{E_j^*} n_q^{(+)}(x_j) & x_j \geq 0, \\ \frac{1}{\pi^2} \sum_j \int p^2 dp \frac{m_j^*}{E_j^*} n_q^{(-)}(x_j). & x_j < 0 \end{cases} \quad (2.20)$$

C. Stellar matter

In stellar matter there are two conditions that have to be fulfilled, namely, charge neutrality and β -stability and they read:

$$\sum_j q_j n_j + \sum_l q_l n_l = 0, \quad (2.21)$$

where $q_{type}, type = j, l$ stand for the electric charge of baryons and leptons respectively and

$$\mu_j = q_j \mu_n - q_e (\mu_e - \mu_\nu), \quad \mu_\mu = \mu_e. \quad (2.22)$$

We have also used the non extensive statistics for the leptons, which enter the calculation as free particles obeying the above mentioned conditions.

The three snapshots of the time evolution of a neutron star in its first minutes of life are given by:

- $\mathcal{S}/n_B = 1, Y_l = 0.3,$
- $\mathcal{S}/n_B = 2, \mu_\nu = 0,$
- $\mathcal{S}/n_B = 0, \mu_\nu = 0,$

where

$$Y_l = \frac{\sum_l n_l}{n_B}, \quad (2.23)$$

which, according to simulations [27], can reach $Y_l \simeq 0.3 - 0.4$. In the present work we are interested in finite temperature systems and hence, most of the results refer to the first two snapshots.

Another aspect of the evolution of compact stars that is worth investigating is the direct Urca (DU) process, $n \rightarrow p + e^- + \bar{\nu}_e$ [28]. It is known that the cooling of the star by neutrino emission can occur relatively fast if it is allowed, what happens when the proton fraction exceeds a critical value x_{DU} [28], evaluated in terms of the leptonic fraction as [29]:

$$x_{\text{DU}} = \frac{1}{1 + (1 + x_e^{1/3})^3}, \quad (2.24)$$

where $x_e = n_e/(n_e + n_\mu)$ is the electron leptonic fraction, n_e is the number density of electrons and n_μ is the number density of muons. Cooling rates of neutron stars seem to indicate that this fast cooling process does not occur and, therefore, a constraint is set imposing that the direct Urca process is only allowed in stars with a mass larger than $1.5 M_\odot$, or a less restrictive limit, $1.35 M_\odot$ [29]. The DU process can also occur for hyperons, if they are taken into account in the EOS. Although the neutrino luminosities in these processes are much smaller than the ones obtained in the nucleon direct Urca process, they play an important role if they occur at densities below the nucleon direct Urca process [30]. The process $\Lambda \rightarrow p + e + \bar{\nu}$, for instance, may occur at densities below the nucleon DU onset. In the next section we also investigate the effects of non extensive statistics on the onset of the DU process.

III. RESULTS

We now calculate and analyze stellar properties obtained with two different values of the non extensive statistics q parameter, namely $q = 1.05$ and 1.14 . Our results are then compared with the ones shown in Ref. [13]. We have chosen values larger than one because lower values produce a slightly softer EoS, which result in lower maximum stellar masses as compared with the standard non-linear Walecka model, as can be seen in Ref. [13]. Since our main goal is to check whether $2M_\odot$ stars can be attained with the help of non extensive thermodynamics when the traditional one fails, we restrict ourselves to values that go in the desired direction. In Ref. [31], the entropic index q , is taken as a fixed property of the hadronic matter with its value determined as $q = 1.14$ from the analysis of p_T -distributions and in the study of the hadronic mass spectrum. The value $q = 1.05$ is used because it is slightly larger than the value used in [13], where the authors used $q = 1.03$ that represents just a small deviation from the standard stellar matter physics.

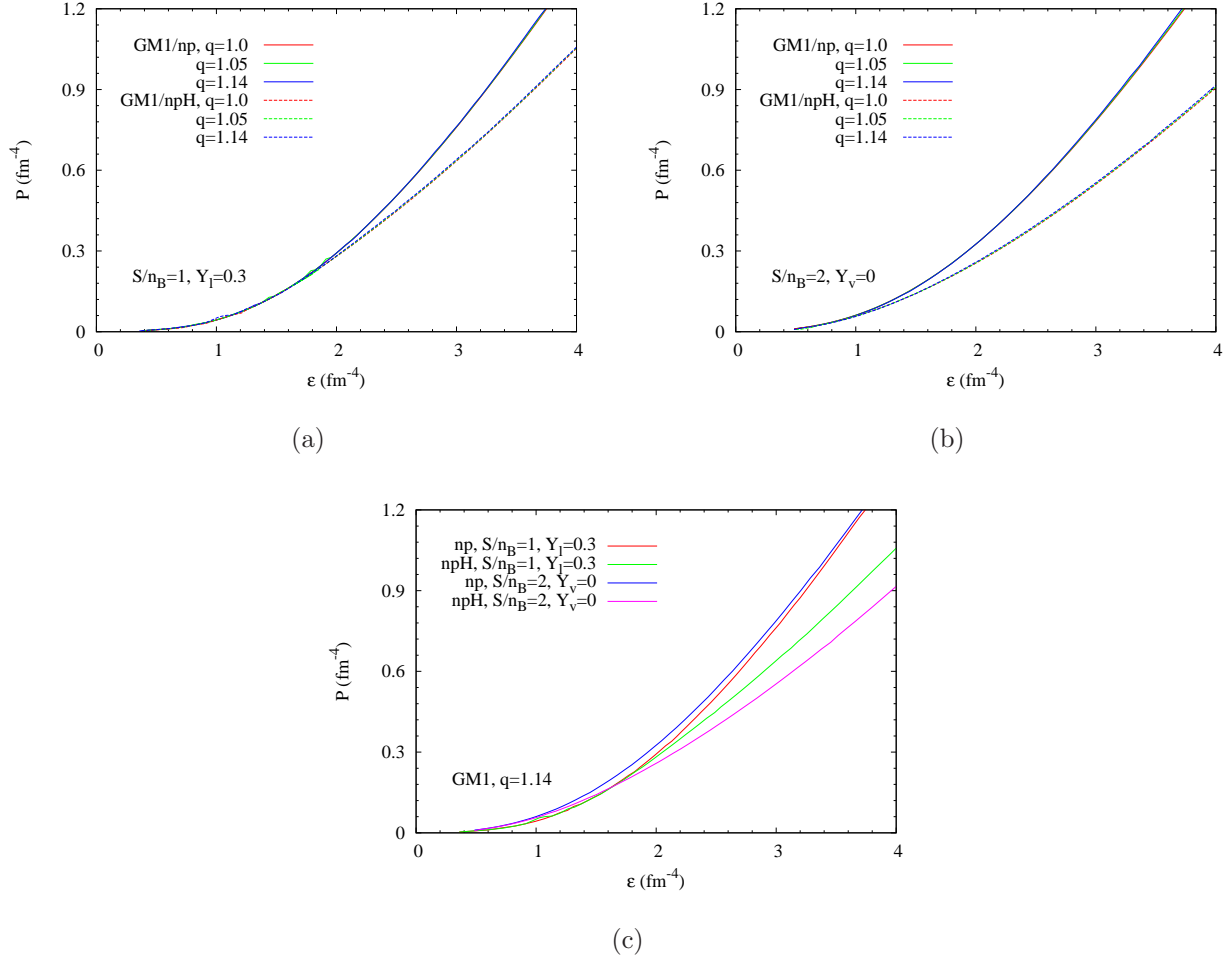


FIG. 1: Equation of state for hadronic matter constituted by nucleons only (np) and including the lightest eight baryons (npH) for different values of q and a) first b) second snapshot of the star evolution c) for $q = 1.14$ only and both snapshots.

In all graphs shown next, the GM1 parametrization was used, but the qualitative results are the same for the IU-FSU parameter set.

We start by showing the EoS for the first two snapshots of the star evolution in Fig. 1 for the cases with nucleons only and also with hyperons. The deviation obtained with non extensive statistics is very small, but larger at high densities for the q -values we have considered, with consequences in the maximum stellar masses, which will be seen later. It is important to observe that, for a fixed q -value, the EoS is slightly harder for $S/n_B = 2, \mu_\nu = 0$ than for $S/n_B = 1, Y_l = 0.3$ when only nucleons are taken as internal neutron star constituents, but it is softer when the hyperons are considered, an effect caused by the inclusion of strangeness in the system.

We then analyze the effects of non extensivity on the internal stellar temperature by plotting the temperature as a function of density again for the first two snapshots of the star evolution in Fig. 2 for both parametrizations investigated in the present work. We clearly see that the temperature decreases with the increase of q , a behavior already expected from the calculations performed in [25] (see, for instance figs. 2 and 6 of that reference). At

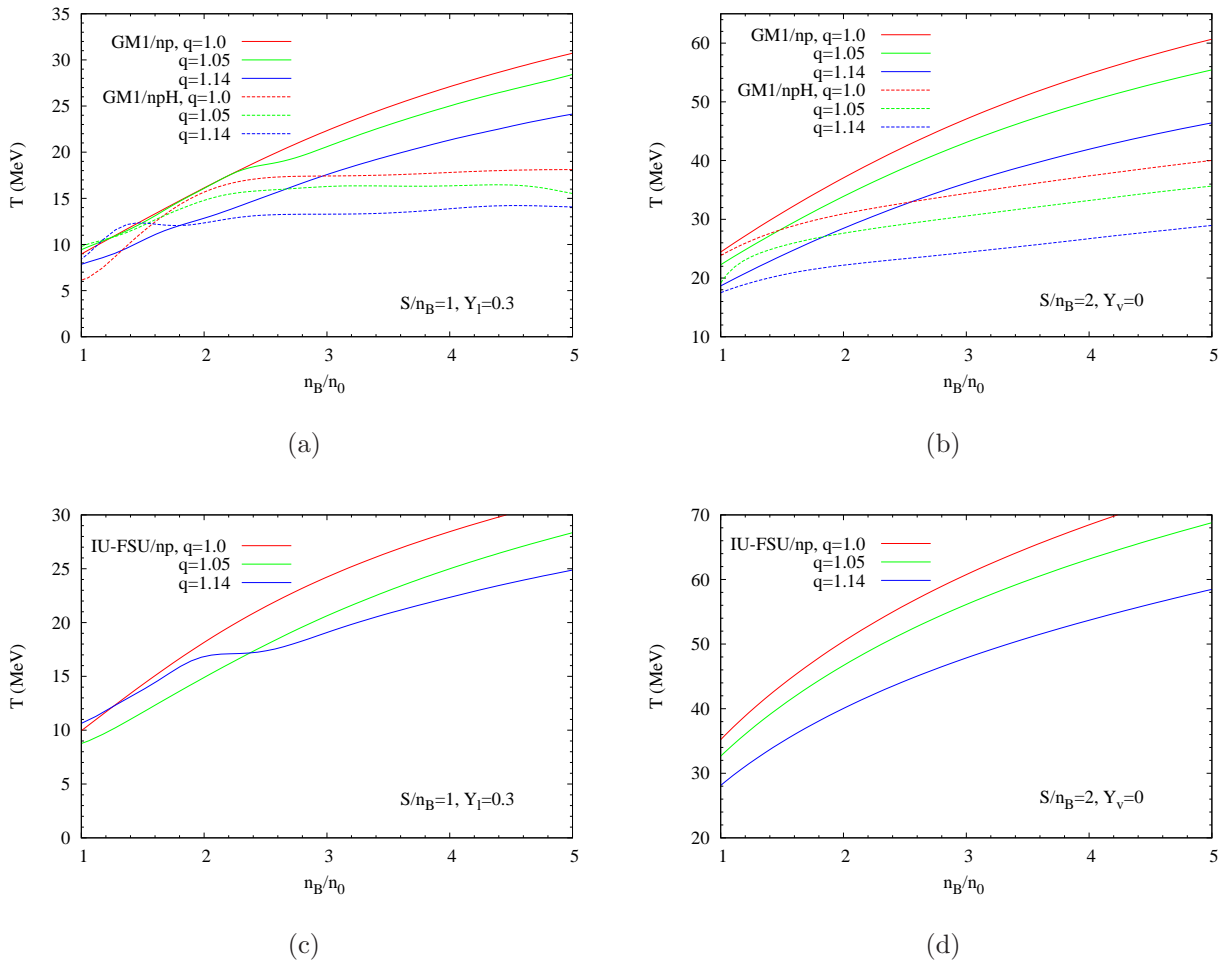


FIG. 2: Temperature as a function of density (in units of nuclear matter saturation density) for different values of q and a) GM1 and first b) GM1 and second c) IU-FSU and first and D) IU-FSU and second snapshot of the star evolution.

densities of the order of 5 times nuclear saturation density, the temperature decreases by approximately 25% in average, with important consequences in the neutrino diffusion during the Kelvin-Helmholtz epoch, when the star evolves from a hot and lepton rich object to a cold and deleptonized compact star. However, in Ref. [13], the behavior is exactly the opposite, i.e. the temperature increases with the increase of the q -value, a result that we do not reproduce.

In order to see how the internal constitution of the star is affected by non extensivity, we plot in Fig. 3 the particle fractions when the hyperons are considered and the related strangeness content in Fig. 4. From these figures, we can see that as q increases, the amount of strangeness decrease, which means that the EoS becomes harder, resulting in larger maximum masses.

In Table II and Fig. 5 we show the main stellar properties obtained from the solution of the Tolman-Oppenheimer-Volkof (TOV) equations [32], which use the EoS just discussed with the GM1 parametrization as input. As expected, from the observation of the EoS, the maximum stellar mass increases with the increase of the q -value. When only nucleons are

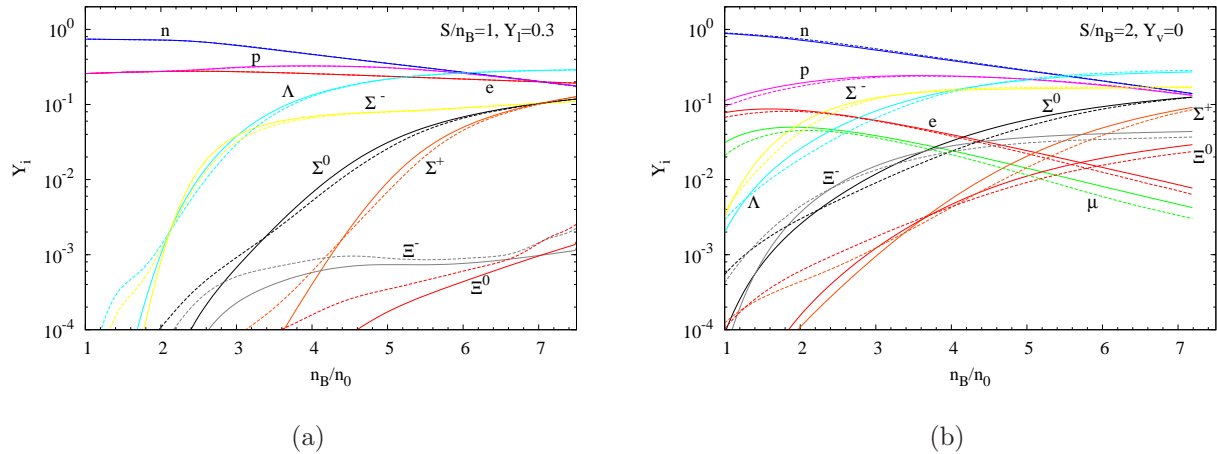


FIG. 3: Particle fractions obtained for a) first and b) second snapshot of the star evolution. We use solid lines for $q = 1.0$ (standard model) and dashed lines for $q = 1.14$.

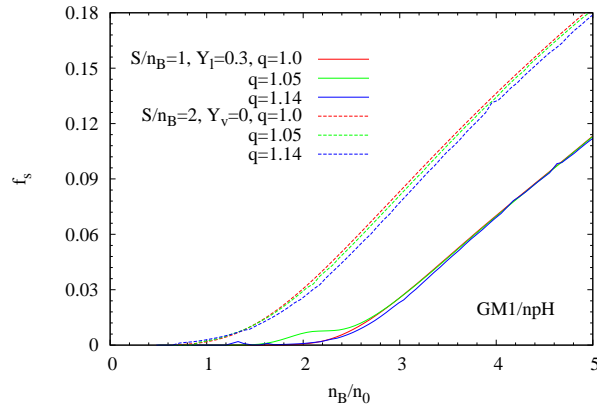


FIG. 4: Strangeness content as a function of density (in units of nuclear matter saturation density) for different values of q and two first snapshots of the star evolution.

taken into account, the maximum stellar masses are obtained during the second snapshot of the star evolution ($\mathcal{S}/n_B = 2$, $\mu_\nu = 0$) and when hyperons are also included, maximum masses come out for $\mathcal{S}/n_B = 1$, $Y_l = 0.3$. This behavior corroborates the findings in Ref. [13]. For the sake of completeness, we also display results obtained at fixed temperature ($T = 30$ MeV) and compare them with the results for a free Fermi gas. In the cases where GM1 was used, there is no obvious pattern with respect to the q -value, i.e. the maximum masses oscillate when the q -value increases. When a free Fermi gas is used, the maximum masses decrease when q increases. As it is well known the huge increase in the maximum masses is due to the inclusion of the nuclear interaction, but we also found a lack of pattern in a system with fixed temperature instead of fixed entropy. In Fig. 5 we plot mass-radius results obtained from the EoS shown in Fig. 1. In these curves the BPS [33] EoS was not included because it is only valid at zero temperature and, as shown in Fig. 2, the temperature at the surface of the star for fixed entropies can be slightly higher. Had we included the BPS EoS, our curves would present a tail towards higher radii, but the differences in the

maximum masses would be minor.

To check the consistency of our results, in Table III we display, for a system with nucleons only, stellar properties obtained with the IU-FSU parametrization. We have not included hyperons because this parameter sets provides too low maximum stellar masses when strangeness is taken into account. The results show that the qualitative conclusions do not depend on the chosen parameter set.

| model | case | q | M_{max} (M_{\odot}) | Mb_{max} (M_{\odot}) | R (Km) | \mathcal{E}_0 (fm^{-4}) |
|----------|---------------------------------------|------|------------------------------|-------------------------------|-----------|---|
| free gas | T=30 MeV, $Y_{\nu} = 0$ | 1.0 | 0.693 | 0.70 | 7.46 | 12.59 |
| free gas | T=30 MeV, $Y_{\nu} = 0$ | 1.05 | 0.689 | 0.70 | 7.30 | 13.48 |
| free gas | T=30 MeV, $Y_{\nu} = 0$ | 1.14 | 0.680 | 0.69 | 7.06 | 14.32 |
| GM1/np | T=30 MeV, $Y_{\nu} = 0$ | 1.0 | 2.10 | 2.37 | 11.48 | 5.83 |
| GM1/np | T=30 MeV, $Y_{\nu} = 0$ | 1.05 | 2.30 | 2.66 | 11.34 | 6.00 |
| GM1/np | T=30 MeV, $Y_{\nu} = 0$ | 1.14 | 2.29 | 2.64 | 11.36 | 5.85 |
| GM1/np | $\mathcal{S}/n_B = 1$, $Y_l = 0.3$ | 1.0 | 2.31 | 2.67 | 11.57 | 5.18 |
| GM1/np | $\mathcal{S}/n_B = 1$, $Y_l = 0.3$ | 1.05 | 2.31 | 2.67 | 11.38 | 5.77 |
| GM1/np | $\mathcal{S}/n_B = 1$, $Y_l = 0.3$ | 1.14 | 2.32 | 2.68 | 11.61 | 5.18 |
| GM1/np | $\mathcal{S}/n_B = 2$, $Y_{\nu} = 0$ | 1.0 | 2.33 | 2.66 | 11.60 | 5.71 |
| GM1/np | $\mathcal{S}/n_B = 2$, $Y_{\nu} = 0$ | 1.05 | 2.33 | 2.68 | 11.64 | 5.62 |
| GM1/np | $\mathcal{S}/n_B = 2$, $Y_{\nu} = 0$ | 1.14 | 2.34 | 2.70 | 11.61 | 5.71 |
| GM1/np | T=0, $Y_{\nu} = 0$ | 1.0 | 2.38 | 2.88 | 11.75 | 5.62 |
| GM1/npH | T=30 MeV, $Y_{\nu} = 0$ | 1.0 | 1.90 | 2.12 | 10.88 | 6.28 |
| GM1/npH | T=30 MeV, $Y_{\nu} = 0$ | 1.05 | 1.90 | 2.11 | 10.73 | 6.78 |
| GM1/npH | T=30 MeV, $Y_{\nu} = 0$ | 1.14 | 1.89 | 2.07 | 10.61 | 6.93 |
| GM1/npH | $\mathcal{S}/n_B = 1$, $Y_l = 0.3$ | 1.0 | 2.10 | 2.39 | 11.40 | 5.69 |
| GM1/npH | $\mathcal{S}/n_B = 1$, $Y_l = 0.3$ | 1.05 | 2.11 | 2.54 | 11.43 | 5.72 |
| GM1/npH | $\mathcal{S}/n_B = 1$, $Y_l = 0.3$ | 1.14 | 2.11 | 2.39 | 11.44 | 5.84 |
| GM1/npH | $\mathcal{S}/n_B = 2$, $Y_{\nu} = 0$ | 1.0 | 1.93 | 2.15 | 10.98 | 6.46 |
| GM1/npH | $\mathcal{S}/n_B = 2$, $Y_{\nu} = 0$ | 1.05 | 1.95 | 2.18 | 11.10 | 6.29 |
| GM1/npH | $\mathcal{S}/n_B = 2$, $Y_{\nu} = 0$ | 1.14 | 1.96 | 2.20 | 11.13 | 6.26 |
| GM1/npH | T=0, $Y_{\nu} = 0$ | 1.0 | 2.00 | 2.32 | 11.51 | 5.96 |

TABLE II:

Finally, in Fig. 6 we plot the onset of the direct Urca process in stellar matter for matter with (dashed lines) and without hyperons (solid lines) in the case where $\mathcal{S}/n_B = 2$, $\mu_{\nu} = 0$. The lines around a y-value of 0.12 refer to x_{DU} and the other lines represent the proton fraction. When the curves cross, we can see the value of the proton fraction and the respective baryonic density. We can see that the line for x_{DU} coincides for the standard model independently of considering or not hyperons. For $q = 1.14$ both curves present a small deviation at large densities. For GM1, the standard density value for which the DU process occurs (at zero temperature and matter without hyperons) is 1.81 times nuclear matter saturation density [23]. When we fix the entropy density to 2 and keep $q = 1$, this value decreases to 1.207 (1.205) n_B/n_0 with (without) hyperons but when we look at the

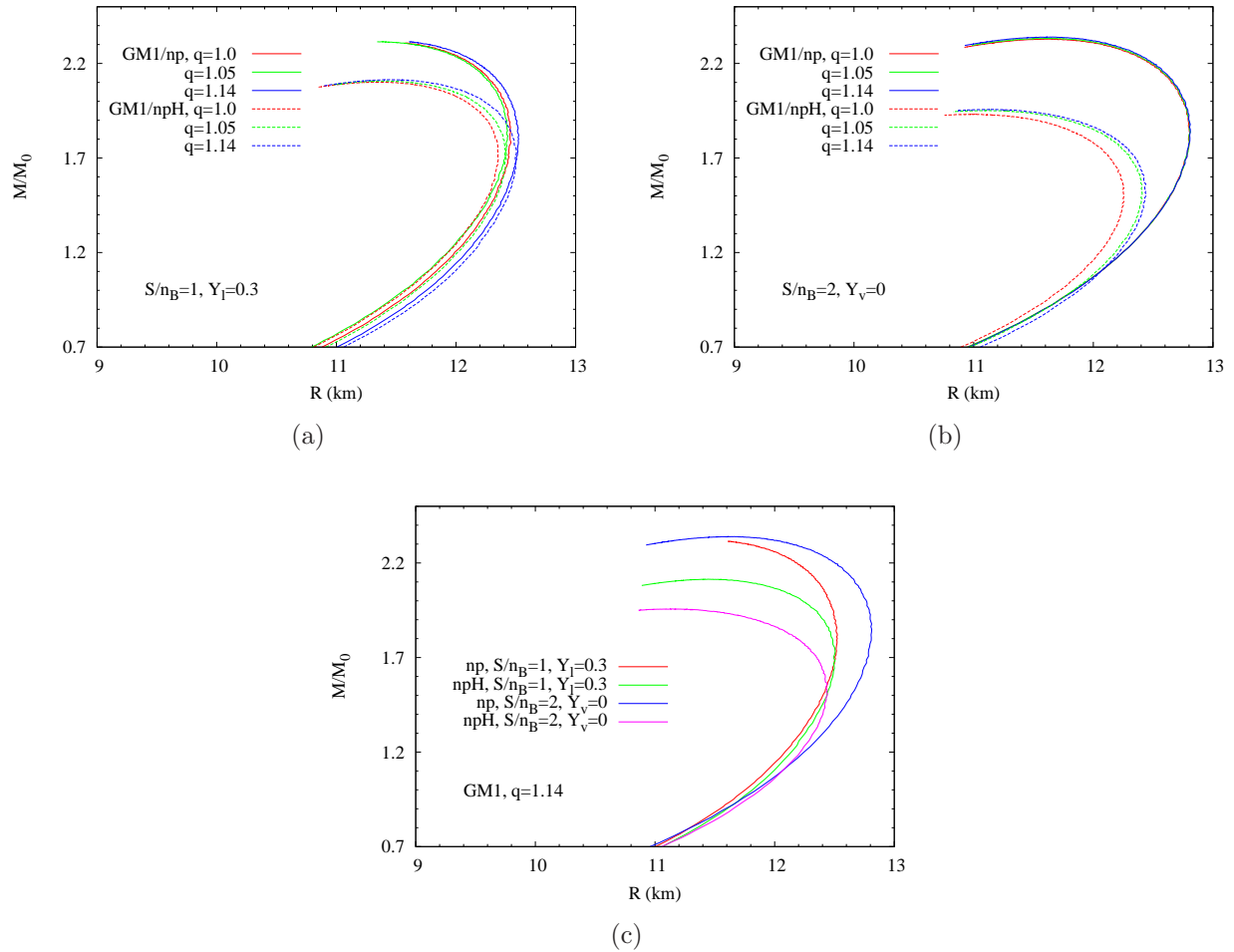


FIG. 5: Mass-radius results obtained from the solution of the TOV equations for hadronic matter constituted by nucleons only (np) and including the lightest eight baryons (npH) for different values of q and a) first b) second snapshot of the star evolution c) for $q = 1.14$ only and both snapshots.

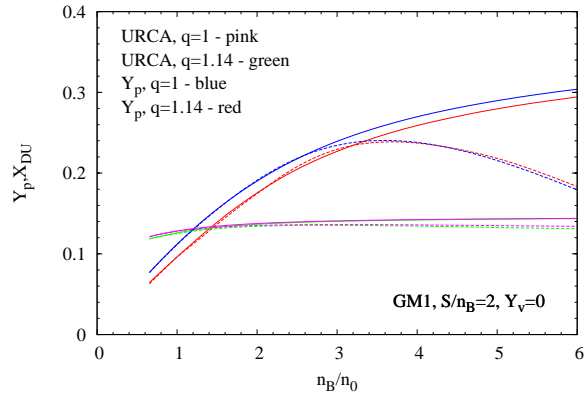
values for $q = 1.14$, we see that the onset of the DU process increases again by approximately 21.5% to 1.423 (1.402) n_B/n_0 with (without) hyperons. The proton fraction that we obtain with nucleons only and with hyperons are coincident for a fixed q -value at low densities and just deviate from each other when other hyperons with positive charge appear. Therefore, if the DU process determines how the star cools down, non extensive statistics certainly affects the cooling rate mechanism.

IV. FINAL REMARKS

We have applied non extensive statistics to calculate equations of state that describe stellar matter with two of the commonly used parametrizations for the non-linear Walecka model, namely GM1 [15] and IU-FSU [16]. We have then fixed two q -values (1.05 and 1.14) and obtained the most important microscopic quantities associated with the equations of state, i.e. particle fractions, strangeness, internal temperature and direct Urca process onset for

| model | case | q | M_{max} (M_{\odot}) | Mb_{max} (M_{\odot}) | R (Km) | \mathcal{E}_0 (fm^{-4}) |
|------------|---------------------------------------|------|------------------------------|-------------------------------|-----------|---|
| free gas | T=30 MeV, $Y_{\nu} = 0$ | 1.0 | 0.693 | 0.70 | 7.46 | 12.59 |
| free gas | T=30 MeV, $Y_{\nu} = 0$ | 1.05 | 0.689 | 0.70 | 7.30 | 13.48 |
| free gas | T=30 MeV, $Y_{\nu} = 0$ | 1.14 | 0.680 | 0.69 | 7.06 | 14.32 |
| IU-FSU/np | T=30 MeV, $Y_{\nu} = 0$ | 1.0 | 1.90 | 2.19 | 10.76 | 6.08 |
| IU-FSU/np | T=30 MeV, $Y_{\nu} = 0$ | 1.05 | 1.90 | 2.19 | 10.71 | 6.46 |
| IU-FSU/np | T=30 MeV, $Y_{\nu} = 0$ | 1.14 | 1.89 | 2.16 | 10.57 | 6.84 |
| IU-FSU/np | $\mathcal{S}/n_B = 1$, $Y_l = 0.3$ | 1.0 | 1.89 | 2.13 | 10.55 | 6.59 |
| IU-FSU/np | $\mathcal{S}/n_B = 1$, $Y_l = 0.3$ | 1.05 | 1.94 | 2.25 | 11.33 | 6.34 |
| IU-FSU/np | $\mathcal{S}/n_B = 1$, $Y_l = 0.3$ | 1.14 | 1.94 | 2.14 | 11.30 | 6.34 |
| IU-FSU/np | $\mathcal{S}/n_B = 2$, $Y_{\nu} = 0$ | 1.0 | 1.97 | 2.19 | 11.29 | 5.86 |
| IU-FSU/np | $\mathcal{S}/n_B = 2$, $Y_{\nu} = 0$ | 1.05 | 1.97 | 2.20 | 11.25 | 5.96 |
| IU-FSU/np | $\mathcal{S}/n_B = 2$, $Y_{\nu} = 0$ | 1.14 | 1.98 | 2.22 | 11.24 | 5.97 |
| IU-FSU/np | T=0, $Y_{\nu} = 0$ | 1.0 | 1.95 | 2.28 | 10.82 | 6.37 |
| IU-FSU/npH | T=0, $Y_{\nu} = 0$ | 1.0 | 1.52 | 1.71 | 10.31 | 6.90 |

TABLE III:



(a)

FIG. 6: Onset of direct Urca process in stellar matter with nucleons only (solid lines) and with hyperons (dashed lines) for the usual Boltzmann-Gibbs statistics ($q=1$) and for $q = 1.14$.

two snapshots of the star evolution. We have confirmed that, as already shown in [13], the equations of state are only slightly modified, but the effects are enough to produce stars with slightly higher maximum masses and these results are common to both parameter sets used. However, contrary to what was obtained in [13], the internal temperature of the stars decreases with the increase of the q -value. Moreover, the direct Urca process is substantially affected by non-extensivity, with consequences on the cooling rates of the stars.

As usually done in the search for macroscopic star properties, the Tolman-Oppenheimer-Volkof equations were then solved for the previously obtained EOS and the macroscopic

quantities were computed. The results were compared with more academic calculations for fixed temperatures and for a free-Fermi gas.

In this work, we have also used the non extensive statistics for the leptons, which enter the calculation as free particles with respect to the strong nuclear interaction, but subject to the conditions of charge neutrality and β -equilibrium. We could have used different q -values for the leptons, but for simplicity, we have opted to use the same values as for the baryons.

ACKNOWLEDGMENTS

This work was partially supported by CNPq (grants 305639/2010-2 and 300602/2009-0), FAPESC (Brazil) under project 2716/2012, TR 2012000344, FAPESP (Brazil) under grant 2013/24468-1, Spanish Plan Nacional de Altas Energías grant FPA2011-25948, Junta de Andalucía grant FQM-225, Generalitat de Catalunya grant 2014-SGR-1450, Spanish MINECO's Consolider-Ingenio 2010 Programme CPAN (CSD2007-00042), Centro de Excelencia Severo Ochoa Programme grant SEV-2012-0234. The research of E.M. has been supported by the Juan de la Cierva Program of the Spanish MINECO, and by the European Union under a Marie Curie Intra-European Fellowship (FP7-PEOPLE-2013-IEF).

-
- [1] J. M. Lattimer and M. Prakash, *Science* **304**, 536 (2004).
 - [2] W. Keil and H. Janka, *Astron. Astrophys.* **296**, 145 (1995).
 - [3] J.A. Pons, S. Reddy, M. Prakash, J.M. Lattimer and J.A. Miralles, *Astrophys. J.* 513, 780 (1999); J.A. Pons, A.W. Steiner, M. Prakash and J.M. Lattimer, *Phys.Rev.Lett.* **86** (2001) 5223-5226.
 - [4] M. Prakash, I. Bombaci, M. Prakash, P. J. Ellis, J. M. Lattimer and R. Knorren, *Phys. Rept.* **280**, 1 (1997).
 - [5] B.D. Serot and J.D. Walecka, *Adv. Nucl. Phys.* **16** (1986) 1.; J. Boguta and A. R. Bodmer, *Nucl. Phys. A* **292**, 413 (1977).
 - [6] N. K. Glendenning, *Compact Stars*, Springer-Verlag, New-York, 2000.
 - [7] P. Haensel, A. Y. Potekhin, D. G. Yakovlev: *Neutron Stars, Equation of State and Structure*, Springer, New York (2006).
 - [8] Paul Demorest, Tim Pennucci, Scott Ransom, Mallory Roberts, and Jason Hessels, *Nature (London)* 467, 1081 (2010).
 - [9] J. Antoniadis et al, *Science* 26, 340 n. 6131 (2013).
 - [10] C. Tsallis, *J. Stat. Phys.* 52 (1988) 479.
 - [11] I. Bediaga, E.M.F. Curado e J.M. de Miranda, *Physica A* 286 (2000) 156.
 - [12] A. Deppman, *Physica A* 391 (2012) 6380; *Physica A* 400 (2014) 207.
 - [13] A. Lavagno and D. Pigato, *Eur. Phys. J. A* (2011) **47**: 52.
 - [14] M. Dutra, O. Lourenço, S.S. Avancini, B.v. Carlson, A. Delfino, D.P. Menezes, C. Providencia, S. Typel and J.R. Stone, *Phys. Rev. C* (2014), accepted, arXiv:1405.3633[nucl-th].
 - [15] N. K. Glendenning and S. A. Moszkowski, *Phys. Rev. Lett.* **67**, 2414 (1991)
 - [16] F. J. Fattoyev, C. J. Horowitz, J. Piekarewicz and G. Shen, *Phys. Rev. C* **82**, 055803 (2010); (arxiv:1008.3030).
 - [17] C. J. Horowitz and J. Piekarewicz, *Phys. Rev. Lett.* **86**, 5647 (2001).

- [18] B. G. Todd-Rutel and J. Piekarewicz, Phys. Rev. Lett. **95**, 122501 (2005); F. J. Fattoyev and J. Piekarewicz, Phys. Rev. C **82**, 025805 (2010).
- [19] Constança Providência, Sidney S. Avancini, Rafael Cavagnoli, Silvia Chiacchiera, Camille Ducoin, Fabrizio Grill, Jerome Margueron, Débora P. Menezes, Aziz Rabhi, Isaac Vidaa, Eur. Phys. J. A (2014) 50:44.
- [20] J. Schaffner-Bielich, A. Gal, Phys. Rev. C **62**, 034311 (2000); J. Schaffner-Bielich, M. Hanauske, H. Stocker and W. Greiner, Phys. Rev. Lett. **89**, 171101 (2002); E. Friedman, A. Gal, Phys. Rep. **452**, 89 (2007).
- [21] Luiz L. Lopes and Debora P. Menezes, Phys. Rev. C **89**, 025805 (2014).
- [22] G. A. Lalazissis, J. König, P. Ring, Phys. Rev. C **55**, 540 (1997).
- [23] Rafael Cavagnoli, Constança Providência, and Debora P. Menezes, Phys. Rev. C **83**, 045201 (2011).
- [24] J.M. Conroy, H.G. Miller and A.R. Plastino, Physics Letters A **374** (2010) 45814584.
- [25] Eugenio Megías, Débora P. Menezes and Airton Deppman, arXiv:1312.7134.
- [26] E. Megias, D. P. Menezes and A. Deppman, arXiv:1407.8044.
- [27] A. Burrows and J. M. Lattimer, Astrophys. J. **307**, 178 (1986).
- [28] J. M. Lattimer, C. J. Pethick, M. Prakash, and P. Haensel, Phys. Rev. Lett. **66**, 2701 (1991).
- [29] T. Klähn, *et al.*, Phys. Rev. C **74**, 035802 (2006).
- [30] M. Prakash, J. M. Lattimer, and C. J. Pethick, Astrophys. J. **390**, L77 (1992).
- [31] L. Marques, E. Andrade-II e A. Deppman, Phys. Rev. D **87**, 114022 (2013).
- [32] R.C. Tolman, Phys. Rev. **55**, 364 (1939); J.R. Oppenheimer and G.M. Volkoff, Phys. Rev. **55**, 374 (1939).
- [33] G. Baym, C. Pethick, and D. Sutherland, Astrophys. J. **170**, 299 (1971).